Stony Brook University

Novel Polymer Thin Film Process Using Supercritical Carbon Dioxide as an Environmentally Green Solvent

A Thesis Presented

by

Peter Gin

to

The Graduate School

in Partial Fulfillment of the

Requirements

for the Degree of

Master of Science

in

Materials Science and Engineering

Stony Brook University

May 2010

Stony Brook University

The Graduate School

Peter Gin

We, the thesis committee for the above candidate for the

Master of Science degree, hereby recommend

acceptance of this thesis.

Tadanori Koga – Thesis Advisor

Assistant Professor, Materials Science and Engineering

Michael Dudley - Chairperson of Defense

Professor, Materials Science and Engineering

Jon Sokolov – Committee Member

Professor, Materials Science and Engineering

This thesis is accepted by the Graduate School

Lawrence Martin
Dean of the Graduate School

Abstract of the Thesis

Novel Polymer Thin Film Process Using Supercritical Carbon Dioxide as an Environmentally Green Solvent

by

Peter Gin

Master of Science

in

Materials Science and Engineering

Stony Brook University

2010

The utilization of supercritical fluids (SCFs) has recently become prominent in a number of polymer processes such as inducing the ordering of block copolymer templates, synthesizing nanoporous material, and spatially distributing nanoparticles in a matrix. For such processes, conventional techniques have relied heavily on the use of toxic organic solvents such as chloroform and toluene. In contrast, certain SCFs, such as supercritical carbon dioxide ($scCO_2$), have been distinguished as a "green" alternative because they are nontoxic, nonflammable, and inexpensive. Furthermore, the easily attainable critical temperature and pressure (T_c=31.3 °C and P_c=7.38 MPa, respectively) make it an ideal solvent choice for polymers that degrade at low temperatures. In the following, I describe the research characterizing the effects of $scCO_2$ on polymer thin films and brushes, specifically their swollen structures. This was achieved using multiple tools including, Neutron Reflectivity, X-Ray Scattering, and various microscopy techniques. I also present and recommend on-going and future work.

Table of Contents

List of Figures

Chapter 1: Introduction

1.1 Supercritical carbon dioxide as a solvent for polymers

Environmentally benign supercritical fluids, such as supercritical carbon dioxide ($scCO_2$) are well regarded and studied as an alternative to conventional organic solvents used in polymer processing. CO_2 is nonflammable and nontoxic in all phases, making it considerably less harmful than solvents in its class. Organic solvents used in polymer processes are often costly to procure and difficult to dispose of, whereas CO_2 is readily available, through practices such as carbon capture, and may be released into the atmosphere or recycled after processing. Supercritical CO_2 has been shown to be a practicable, green choice for processes such as inducing self assembly of block copolymer templates [1], formation of nanoporous films [2, 3], and spatial implantation of nanoparticles in polymer matrices [4], of which are traditionally achieved using organic solvents or excess thermal energy. Supercritical fluids are known to produce annealing type effects on polymer thin films at modest conditions. [5, 6] The supercritical phase occurs as a result of elevated temperature and pressure above their respective critical points, as seen in Fig. 1-1, at which point the fluid exhibits highly penetrable gas-like diffusivity characteristics coupled with liquid-like density. For CO_2, the critical temperature, Tc is 31.3 C and critical pressure, Pc is 7.38 MPa. Comparatively, the supercritical phase for CO_2 is more readily attainable than other fluids; i.e. H_2O (Tc = 374.2, Pc = 22.06) [7]. Variation in temperature and pressure of supercritical fluids enables the ability to control density dependent solvent properties [8]. Consequently, only small manipulations are necessary to induce physical as well as thermodynamic and transport properties of the polymer. This highly tunable nature effectively makes supercritical fluids a "universal" solvent for polymers. Because of the novel features of $scCO_2$, we wish to further develop a better understanding of the processing abilities of this green solvent, especially for polymer thin films. We will try to achieve this by systematically testing and measuring: (i) the physical changes induced by $scCO_2$ for various polymer systems, (ii) the effect of $scCO_2$ on the film's thermal and mechanical properties, and (iii) the effectiveness of additives, i.e. pre-solvents and cross-linkers for enhancing the abilities of $scCO_2$. In doing so, it may further propel SCFs as a more valid environmentally friendly alternative to organic solvents for polymer thin film processing.

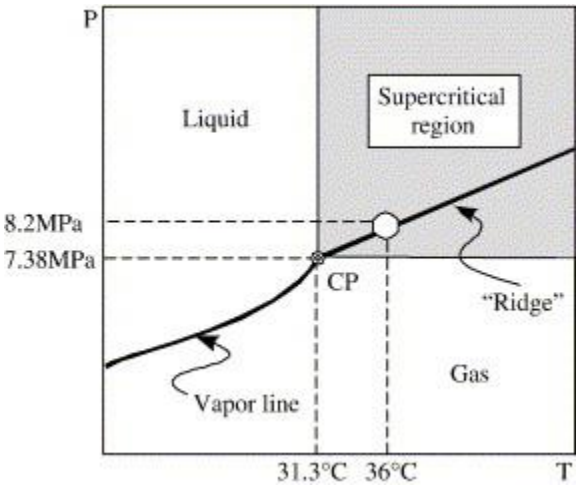

Figure 1-1. The location of the supercritical regime and density fluctuation ridge for CO_2

1.2 Solvent quality of supercritical carbon dioxide for polymers

Good miscibility between the supercritical fluid and polymer enhances swelling effects. "CO_2-philic" polymers are known to have favorable free energies of mixing with

CO_2. As a result, the compound can be dissolved in CO_2 under relatively moderate conditions (T < 100 °C and P < 50 MPa) [18]. When exposed to $scCO_2$, this class of polymer exhibits a significant degree of swelling. Unfortunately, the class of polymers that are CO_2-philic is very limited. Highly fluorinated or silicone based polymers are examples of just a hand-few of polymers that can be processed with CO_2 easily. The effectiveness of a solvent is determined by its ability to adequately dissolve one material while leaving other materials unaffected. To effectively dissolve a polymer, the solvent must overcome van der Waals forces due to intermolecular polarities in the long chained molecules. This is accomplished when both the solvent and solute are miscible with one another due to strong molecular attractions. Weak attraction to the solvent will not cause the polymer molecules to separate, as they are more attracted to each other. Solubility may be presented using numerous scales. The most applicable and commonly used system is the Hildenbrand solubility parameter. The Hildenbrand solubility parameter ∂ is a numerical value defined as the square root of the cohesive energy density

$$\partial = \sqrt{c} = \sqrt{\frac{\Delta H - RT}{V_m}} \qquad (1.1)$$

where c is the cohesive energy density, ΔH is the heat of vaporization, R is the gas constant, T is the temperature, and V_m is the molar volume. This numerical system allows for the grouping of similar solvents of comparable internal energies. Components with similar Hildenbrand solubility parameters will be attracted to one another and would be miscible. Consequently, a group of solvents with similar solubility parameters may dissolve the same polymer. Polymers which cannot be dissolved exhibit swelling behavior in precisely the same manner. The extent of swelling in polymers is greatest when the differences in the Hildenbrand values are low. Supercritical CO_2 as a solvent is not able to dissolve polymers but as a result of molecular attraction to the polymer can produce this swelling effect [19].

1.3 "Density fluctuating" supercritical carbon dioxide

According to the molecular dynamics simulation of a two-dimensional Lennard–Jones fluid, $scCO_2$ is composed of high-density and low-density regions, resulting in density fluctuations, as seen in Fig. 1-2 [24]. As the critical point of a fluid is approached, the correlation length and the isothermal compressibility, κ_T, deviate [25]. The density fluctuations, $\langle(\Delta N)^2\rangle / \langle N\rangle$, witnessed can then be expressed by using κ_T:

$$\langle(\Delta N)^2\rangle/\langle N\rangle=(N/V)\kappa_T k_B T, \qquad (1.2)$$

where N is the number of molecules in the corresponding volume V, k_B is the Boltzman constant, κ_T is the isothermal compressibility, and T is the thermodynamic absolute temperature [25]. If the κ_T values are known as a function of temperature and pressure, we can describe the thermodynamic behavior in $\langle(\Delta N)^2\rangle / \langle N\rangle$ of SCFs. Fig. 1-3a shows the $\langle(\Delta N)^2\rangle / \langle N\rangle$ values of CO_2 under the isothermal conditions near the critical point. The κ_T values

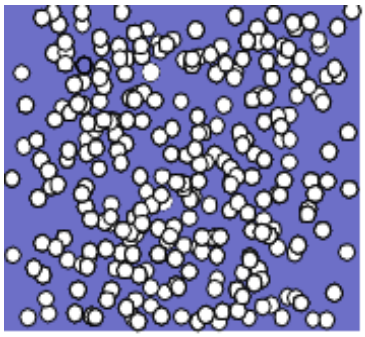

Figure 1-2. Molecular distribution in SCFs shows density fluctuations

were obtained using the equation of state of CO_2 given by Huang et al. [26]. From the figure we can see that the characteristic features of the density fluctuations in the supercritical region are: (i) there is a peak in each lateral curve, (ii) the amplitude of the fluctuations seems to diverge as the critical point is approached, and (iii) the width of the peak broadens with increasing pressure [27]. By extrapolating, the locus of the peaks in the $<(\Delta N)^2> / <N>$ curves forms a "ridge" of the density fluctuations, as shown in Fig. 1-1. The ridge separates the more liquid-like and more gas-like regimes in the supercritical region. Along the ridge, the maximum or minimum of various physical quantities of SCFs, related to the second derivatives of the Gibbs free energy, such as isothermal compressibility, thermal conductivity, and partial molar volumes, is witnessed.

1.4 Novel features of density fluctuating $scCO_2$ for polymer thin films

1.4.1 Processing amorphous polymer thin films using Supercritical Carbon Dioxide

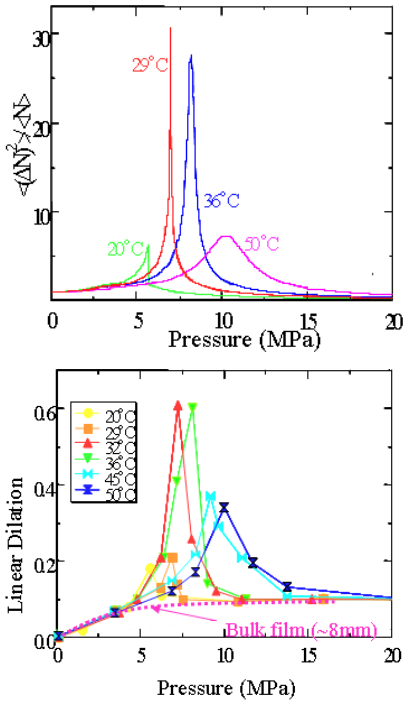

Figure 1-3. **(a)** Maximum density fluctuations of CO_2 under isobaric conditions corresponds directly to **(b)** the maximum linear dilation

Supercritical CO_2 has recently garnered much interest as a processing technique of polymer thin films. Polymer thin films have been investigated and utilized as a medium by the microelectronics industry for such processes as low dielectric inter-layers, and photoresist coating for patterning in the photolithography process [9]. It has been shown that by manipulating the chemistry of polymer it is possible to control the thickness of film on the nanometer scale. This controllability indicates the possibility of creating polymer thin films on the order of the chain's radius of gyration, Rg, where molecular interactions can account for changes in the properties of the material. Processing with $scCO_2$ at this extent generates more appreciable results as compared to bulk polymers, due to excess CO_2 in polymer thin films [10, 11]. Anomalous behavior is especially noticeable in the vicinity of the CO_2 critical point, where compressibility is large [12, 13]. Anomalous maxima in adsorption and swelling in thin films are known to be as a result of long range density fluctuations of CO_2. Wang et al. explored the anomalous sorption phenomena analytically at the surface of polydimethylsiloxane (PDMS) films using numerical methods [13]. Anomalous swelling in $scCO_2$ was investigated by Sirard et al. using in situ spectroscopic ellipsometry on PDMS and polymethyl methacrylate (PMMA) [11]. Our previous work explored swelling maxima of amorphous polymer thin films supported on inorganic substrates using in situ neutron reflectivity [10, 12]. From the studies, it has been concluded that the anomalous swelling behavior occurs along the density fluctuation ridge [14, 15]. At ridge conditions, excess CO_2 at the polymer / CO_2 interface can diffuse readily through amorphous films of thicknesses less than 10Rg causing anomalous swelling. Swelling in the films resulted in low density films free of any visible voids.

Using neutron reflectivity, concentration profiles were obtained for amorphous polymers of varying CO_2 miscibility. Analysis of the profiles reveals that anomalous swelling occurs primarily as result of interfacial effects, namely at the polymer/ CO_2 interface.

1.4.2 Polymer Brushes in density fluctuating Supercritical Carbon Dioxide

Similar studies were performed to investigate the swelling behavior of end-grafted brush polymers [16-18]. Polymer brushes are formed if the monomer density in an end-grafted polymer layer becomes sufficiently large causing the chains to stretch away from the surface. Because one end of the polymer chain is tethered to the substrate, Koga et al explored whether this confinement of the chain ends leads to a different conformation than that of the free-chain situation in $scCO_2$. The equilibrium brush structure is determined by a balance between the interactions that promote stretching of the polymer chains and the associated loss of chain conformational entropy [17]. In addition, because polymer brushes can stretch without being removed from the substrate even in a good solvent, the solvent quality of density fluctuating $scCO_2$ could be investigated on the basis of the chain conformation perpendicular to the grafting surface [18]. Using in-situ NR, a quantitative study of the solvent quality of $scCO_2$ was performed near the locus of maximum density inhomogeneity. The NR study showed that the solvent quality of density fluctuating $scCO_2$ for deuterated polystyrene (dPS) was still poor at the ridge condition where the excess swelling (~30%) occurred.

1.4.3 The Effect of Polymer Elasticity and Crystallinity on Swelling

From the theories of Flory and Huggins, polymer chain length and chain flexibility, significantly influence the entropy of mixing. The mixing of polymers with solvents is said to be more favorable as the chain size decrease because the entropy of mixing is greater. Flexible chains were also described as producing greater entropy of mixing, and stiff chains tended towards phase separation in mixtures. Similarly, comparisons of swelling behavior between glassy and rubbery amorphous polymer thin films have shown that the magnitude of anomalous swelling subsequent to $scCO_2$ exposure is also a function of initial elasticity [12]. Accordingly, it is believed that to witness maximum density dilation, the polymer must exist in a rubbery state. In crystalline polymers, it was found that the extent of crystallization can affect anomalous behavior. Li et al. reports an unusually small degree of swelling in crystalline polyethylene oxide (PEO) analogous to the higher solubility of CO_2 in amorphous PEO reported by Weidner et al [20, 21]. The anomalous maxima, though evident, is significantly suppressed by the crystalline structure. The ability for $scCO_2$ to swell polymer thin films is a function of the fluid's ability to fully penetrate the film at the interface and diffuse throughout. For crystalline thin films, its rigid structure is believed to retard this behavior, thus swelling is less pronounced.

1.5 Research Objectives

As discussed in the aforementioned, the degree of anomalous swelling is affected by the confinement of the polymer, its miscibility with the solvent, polymer elasticity, and the crystal structure. There is currently an incomplete understanding of how each factor influences the swelling phenomena. The objectives of this research are therefore to

systematically develop a better understanding of the effects of $scCO_2$ on a variety polymer thin films and brushes using three approaches: (i) study the conformation of a confined CO_2-philic fluorinated polymer in $scCO_2$, (ii) enhancing the swelling of immiscible semi-crystalline polymer thin films in $scCO_2$ using an intermediate solvent, (iii) tuning the density-dependent properties of the polymer by introducing molecular level porosity.

When a polymer film is exposed to $scCO_2$ at the onset of the critical point, at the density fluctuation ridge, anomalous swelling will occur. For polymer brushes, of which the chain ends are chemically grafted to a solid surface, the confinement of the ends may lead to a different conformation than of the non-tethered situation in $scCO_2$. Koga et al. showed that the anomalous swelling of glassy polymers brushes in immiscible $scCO_2$ is similar to that observed in the unanchored analogous, even at the density fluctuation ridge [18]. Ivkov et al. showed that by using a theta solvent, the degree of swelling in the polymer films are enhanced compared to a poor solvent [22]. To understand systematically the effect of solvent quality on excess swelling in polymer brushes, we explore the conformation of CO_2-philic fluorinated polymers at varying solvent qualities, and at the density fluctuation ridge.

In order to increase the swelling ability of crystalline polymers, it is necessary to improve the polymer-CO_2 miscibility. In most crystalline and semi-crystalline polymers the amount of intermolecular forces holding the molecules together are much greater than their attraction to $scCO_2$. It is possible though to use a secondary medium as a precursor to $scCO_2$. According to solvent mixture theory, the Hildenbrand value of a mixture of two solvents is the average of each individual solvent by volume [19]. Rather than creating a mixture of solvents, it may be possible to utilize each solvent individually to achieve the desired result.

Polymer thin films exhibit thickness dependent properties such as glass transition temperature, wetting, and phase equilibrium [20, 23]. Properties such as diffusivity, viscosity, and dielectric constant, on the other hand, are density dependence. Density fluctuating $scCO_2$ has the ability to modify both the thickness and the density of polymer thin films. High penetrable and dense CO_2 at ridge conditions can diffuse throughout the film enabling the polymer the swell. The swollen structure of the film can be captured by using a quenching process. Highly pressurized CO_2 is removed by quick evaporation into the atmosphere leaving the polymer films in a vitrified state. Consequently, the thickness of the processed films is increased. Molecular scale porosity within the film is also a byproduct of the caused by the inhomogeneous concentration of CO_2 at the ridge. The finite porosity has been shown to effectively lower the density of the polymer film.

1.6 Research Approach and Organization

This report discusses novel methods for utilizing $scCO_2$ for the processing of polymer thin films and brushes. We investigated a number of polymer systems (amorphous homopolymer, semi-crystalline homopolymer, and brush polymer) supported on silicon substrates fabricated using different methods, including spin casting and chemical vapor deposition. Thicknesses of films and brushes were typically below 1000 Angstroms of various molecular weights.

Polymer systems were exposed to $scCO_2$ in a high pressure cell. The body of the high-pressure cell was machined from 4340 steel. Sapphire was selected for the optical window material because of high transparency for neutrons. Furthermore, sapphire has high tensile strength (elastic limit 448 MPa), resistance to corrosion, high-energy damage threshold, and low absorbance. Two cylindrical sapphire windows (2.4 cm in thick, o.d. 5 cm) were installed for transmitting the incident beam and for receiving the reflected beams. The sealing was achieved by a combination of Teflon and a nylon gasket placed between the sapphire windows. The cell had a volume of about 10 mL and a maximum pressure rating of 140.0 MPa. CO_2 used in this study has a purity of 99.9%. CO_2 was loaded into the cell by means of a hand-operated syringe pump (HIP Equip.) to the desired pressure. Prior to pressurization, the air space is purged with the gas at low pressure. Figure 2b shows the general experimental arrangements for experiments. CO_2 pressure inside the cell was monitored by using an OMEGADYNE pressure transducer (TH-1) with a pressure gauge meter (INFS-0001-DC1). The temperature of the cell was controlled by a temperature controller (CAL Controls) equipped with heaters that were installed on the outer side of the cell and a thermocouple (Rama Co.). The temperature of the system was controlled with an accuracy of $\pm 0.1\ ^{\circ}C$, and the stability of pressure during the measurements was less than ±0.2%.

The behaviors of the polymers were investigated using high energy neutron and X-ray spectroscopic techniques. For the polymer brush systems, in situ neutron reflectivity was used to project the effects of density fluctuations on the solubility of $scCO_2$. The conformation and swelling of the polymer were also investigated to determine the role of CO_2-philicity in processing with $scCO_2$. From the reflectivity profiles, thickness, scattering length density, and interfacial width/ roughness, of the polymer could be determined. Density profiles were modeled to project changes in polymer concentration as a function of the CO_2 solvent quality.

Various X-ray techniques were utilized to examine polymer thin films prior to and subsequent to $scCO_2$ exposure. The quick evaporation of CO_2 from the high pressure cell to atmospheric pressure allows us to maintain the film's swollen structure. The films are stable at room temperature which allows us to use techniques such as x-ray reflectivity and grazing incidence diffraction to probe the properties enhanced by $scCO_2$. X-ray reflectivity profiles provide insight into deviations of the film's thickness, density, and interfacial properties after exposure to $scCO_2$.

For our investigations on the enhancing the density dependent properties of polymer thin films, spectroscopic ellipsometry is employed. The ellipsometry measurements yielded changes in the film's thickness and the polymer's index of refraction (nf). The difference witnessed in nf can be used to correlate changes in the density dependent properties of the polymer.

Atomic force microscopy (AFM) is a powerful tool used to probe the topography of films. Three-dimensional topographical images of the films were produced to insure that no void or other dewetting structures were formed. From the images, cross-sectional analysis and surface roughness measurements were also performed to visually inspect the effects of $scCO_2$ on the film quality.

Chapter 2 of this report focuses on our neutron reflectivity study of CO_2-philic brush polymers. Because fluorinated polymers are miscible in CO_2, an in situ study is ideal to examine the configuration of polymer chains while exposed to the solvent. The

tunability of super critical fluids allows us to adjust the solvent quality of CO_2 such that a comparison with recent theory can be performed. Variation of the brush height with solvent quality is modeled using experimental measures of density profiles. Density fluctuating $scCO_2$ is also investigated to determine if concentration inhomogeneity affects solvent quality.

The studies in Chapter 3 examine the prospect of using an organic solvent in conjunction with $scCO_2$ to process and enhance swelling in crystalline and semi-crystalline polymer thin films. Crystal structure is evaluated using GID. An organic solvent is chosen based on its solubility with the polymer. Film thicknesses were characterized by XR before and after processing. Density profiles extracted from the reflectivity are examined to determine density changes in the film. We report the ability of $scCO_2$ to create low density polymer thin films by introducing molecular level porosity to semi-crystalline polymers. This study focuses on density dependent properties, specifically, index of refraction and dielectric constant. We examine spectroscopic ellipsometry measurements for changes in refractive index induced by $scCO_2$. The ability to create ultra-low dielectric constant thin films is also examined. The effect of molecular level porosity on the mechanical and thermal properties of the low density film is studied using Shear Modulation Force Microscopy (SMFM) and Mass Spectroscopy respectively.

Finally, the major conclusions from the above research are presented in Chapter 4. Future work regarding the stability of polymer thin films after processing with $scCO_2$ at high temperatures is discussed. The unified $scCO_2$ process will also be examined for its validity to enhance swelling in amorphous glassy polymer films.

1.7 References:

[1] Y. Li, X. C. Wang, I. C. Sanchez, K. P. Johnston, P. F. Green, *Journal of Physical Chemistry B* **2007**, *111*, 16.

[2] L. Meli, Y. Li, K. T. Lim, K. P. Johnston, P. F. Green, *Macromolecules* **2007**, *40*, 6713.

[3] J. A. Lubguban, S. Gangopadhyay, B. Lahlouh, T. Rajagopalan, N. Biswas, J. Sun, D. H. Huang, S. L. Simon, A. Mallikarjunan, H. C. Kim, J. Hedstrom, W. Volksen, R. D. Miller, M. F. Toney, *Journal of Materials Research* **2004**, *19*, 3224.

[4] H. Wakayama, Y. Fukushima, *Industrial & Engineering Chemistry Research* **2000**, *39*, 4641.

[5] Y. P. Handa, J. Roovers, F. Wang, *Macromolecules* **1994**, *27*, 5511.

[6] H. Yokoyama, K. Sugiyama, *Langmuir* **2004**, *20*, 10001.

[7] T. Koga, Y. S. Seo, J. L. Jerome, S. Ge, M. H. Rafailovich, J. C. Sokolov, B. Chu, O. H. Seeck, M. Tolan, R. Kolb, *Applied Physics Letters* **2003**, *83*, 4309.

[8] T. Koga, *Kobunshi Ronbunshu* **2004**, *61*, 458.

[9] E. K. Lin, C. L. Soles, D. L. Goldfarb, B. C. Trinque, S. D. Burns, R. L. Jones, J. L. Lenhart, M. Angelopoulos, C. G. Willson, S. K. Satija, W. L. Wu, *Science* **2002**, *297*, 372.

[10] T. Koga, Y. S. Seo, X. Hu, K. Shin, Y. Zhang, M. H. Rafailovich, J. C. Sokolov, B. Chu, S. K. Satija, *Europhysics Letters* **2002**, *60*, 559.

[11] S. M. Sirard, K. J. Ziegler, I. C. Sanchez, P. F. Green, K. P. Johnston, *Macromolecules* **2002**, *35*, 1928.

[12] T. Koga, Y. S. Seo, K. Shin, Y. Zhang, M. H. Rafailovich, J. C. Sokolov, B. Chu, S. K. Satija, *Macromolecules* **2003**, *36*, 5236.
[13] X. C. Wang, I. C. Sanchez, *Langmuir* **2006**, *22*, 9251.
[14] K. Nishikawa, T. Morita, *Chemical Physics Letters* **2000**, *316*, 238.
[15] K. Nishikawa, I. Tanaka, Y. Amemiya, *Journal of Physical Chemistry* **1996**, *100*, 418.
[16] A. Karim, S. K. Satija, J. F. Douglas, J. F. Ankner, L. J. Fetters, *Physical Review Letters* **1994**, *73*, 3407.
[17] S. M. Sirard, R. R. Gupta, T. P. Russell, J. J. Watkins, P. F. Green, K. P. Johnston, *Macromolecules* **2003**, *36*, 3365.
[18] T. Koga, Y. Ji, Y. S. Seo, C. Gordon, F. Qu, M. H. Rafailovich, J. C. Sokolov, S. K. Satija, *Journal of Polymer Science Part B-Polymer Physics* **2004**, *42*, 3282.
[19] J. Burke, in *The book and Paper Group Annual*, Vol. 3, The Oakland Museum of California, Austin **1984**, 13.
[20] Y. Li, E. J. Park, K. T. L. Lim, K. P. Johnston, P. F. Green, *Journal of Polymer Science Part B-Polymer Physics* **2007**, *45*, 1313.
[21] E. Weidner, V. Wiesmet, Z. Knez, M. Skerget, *Journal of Supercritical Fluids* **1997**, *10*, 139.
[22] R. Ivkov, P. D. Butler, S. K. Satija, L. J. Fetters, *Langmuir* **2001**, *17*, 2999.
[23] C. L. Soles, J. F. Douglas, R. L. Jones, W. L. Wu, *Macromolecules* **2004**, *37*, 2901.
[24] S. C. Tucker, *Chemical Reviews* **1999**, *99*, 391.
[25] H. E. Stanley, *Introduction to Phase Transition and Critical Phenomena*, Oxford University Press, Oxford **1971**.
[26] M. H. L. F.H. Huang, K.E. Starling and F.T.H. Chung, *J Chem Eng Jpn* **1985**, *18*, 490.
[27] T. Koga, J. Jerome, M. H. Rafailovich, B. Chu, J. Douglas, S. Satija, *Advances in Colloid and Interface Science* **2006**, *128*, 217.

Chapter 2: Swollen Structures of CO_2-philic Polymer Brushes in Density Fluctuating Supercritical Carbon Dioxide.

The utilization of supercritical carbon dioxide ($scCO_2$) has recently become prominent in a number polymer processes, and has been distinguished as a "green" alternative to conventional techniques using toxic organic solvents. We subsequently established new methodology that facilitates enhanced swelling, i.e. as much as 30-60 %, in a wide variety of polymer thin films, specifically when the bulk polymers have very poor miscibility with CO_2. However, it is unclear whether this anomalous behavior, which occurs within a narrow set of operating conditions, called the "density fluctuation ridge", is specific for CO_2 immiscible polymers or if it can be witnessed in polymers of different inherent miscibilities. We aim to further apply our technique to "CO_2-philic" polymers in order to determine the role of inherent miscibility on the extent of excess swelling in polymer thin films. In this presentation, we describe the use of in situ neutron reflectivity (NR) to examine polymer enhanced swelling in density fluctuating $scCO_2$. We report the swelling behavior of semi-crystalline and amorphous poly {2-(perfluorooctyl)ethyl acrylate} brushes, which are not only highly miscible with $scCO_2$ but also an ideal system for the study of chain conformations by varying the solvent quality of $scCO_2$.

2.1 Introduction

A significant challenge that hinders the prospect of $scCO_2$ as a valid alternative to organic solvents is that many nonvolatile compounds are immiscible in CO_2. CO_2 has no dipole moment and has a low polarizability per volume which causes little interaction between the compounds[1]. These weak repulsive forces are not sufficient enough to overcome the attractive van der Waals forces between the molecules to induce solvation. One approach to enhance CO_2 solubility to induce larger repulsive forces between the polymer chains making the contact with solvent more favorable. Densely packed polymer chains will repel from each other breaking van der Waals forces. A stable method for creating compact polymer layers is to permanently graft the chain ends to a substrate surface[2]. Once the monomer packing density becomes sufficiently large at the grafted surface, the polymer chains will stretch to avoid contact with neighboring chains and form a polymer brush.

The equilibrium polymer brush conformation is ultimately determined by interactions that promote chain stretching, which dissects the van der Waals forces between the particle cores, and favorable free energies of mixing with the solvent. Polymers with low cohesive energy densities and low surface tension are said to be CO_2-philic because their free energies of mixing are negative[3]. This limited class of polymers includes fluorinated polymers. This high solubility of fluorinated polymers in both liquid and supercritical CO_2 provides an excellent opportunity to examine the extent of enhanced solubility of end-grafting fluorinated polymers brushes. The combination of repulsive forces between the densely tethered chains and the tendency of the fluorinated polymer to maximize favorable contacts with good solvent molecules should contribute to increase solubility in $scCO_2$. The best marker for the enhancement will be an increase in the swelling behavior compared to the free-chain situation. Neutron reflectivity (NR) will be used to evaluate this change. The large penetration depth and resolution inherent with neutrons makes NR an ideal tool for determining the *in situ* thickness, composition, and interfacial structure of polymer thin films immersed in fluids or gases under high pressure in thick-walled vessels. In addition, the segment density profile can be projected using NR. Previous work has shown that both the magnitude of the brush height and the approximated fit of the density profile are good indicators of solvent quality. Karim et al. showed that Toluene is a good solvent for end grafted polymer PS-SiCl3 using neutron reflectivity. The solvent quality of $scCO_2$ for brush polymers was also investigated. Koga et al. showed that $scCO_2$ is poor solvent for deuterated-PS at various CO_2 densities including at the density fluctuation ridge. At high CO_2 density conditions, Sirard et al. was able to reach a near theta solvent for deuterated-PDMS.

For this study, poly[2-(perfluorooctyl)ethyl acrylate] (PFA-C_8) was end grafted onto a clean silicon substrate. The high solubility of PFA-C_8 in $scCO_2$ can be attributed to the weak intermolecular interactions associated with the high electronegativity and low polarizability of the perfluoroalkyl groups. The polymer has a glass transition temperature of 52 ◦C and exhibits a mesomorphic/isotropic phase transition temperature because of the long fluoroalkyl side chain crystallization at ~77 ◦C [4]. Recent studies have shown the viability of both liquid and $scCO_2$ as a coating solvent for PFA-C_8. Kim et al. were able to deposit highly uniform films of low RMS roughness (≈2 nm) with thicknesses in the range of 7–30 nm. They were able to demonstrate that dramatic differences between the solubility properties of different polymers can affect the

morphology and uniformity of films formed using liquid and supercritical carbon dioxide as a solvent. Highly uniform films of PFA-C_8 can be used in a wide array of applications including biocompatible coatings for medical devices, resists for bio-array device fabrication, or in the area of self-cleaning applications.

The objective of this chapter is to study the swelling behavior of fluorinated brush polymers at different solvent qualities and at the density fluctuation ridge. The highly tunable nature of supercritical fluids allows it to transition continuously from gas-like to liquid-like through modest changes in temperature and/or pressure. Because polymer brushes can stretch without being removed from the substrate, tuning the solvent quality of CO_2, by varying the concentration, allows us to manipulate the chain extension and conformation. Furthermore, because of the high CO_2-philicity of fluorinated polymers, the solvent range can extend from non-solvent conditions to above theta solvent, as the density of CO_2 increases. We further examine the solvent quality of CO_2 along the density fluctuation ridge, where the maximum solvent concentration inhomogeneity is defined, on the basis of determining the effect on the absolute solubility of $scCO_2$. In situ NR experiments were used to measure the thickness and surface concentration profiles of the fluorinated brushes as a function of the solvent quality.

2.2 Experimental Section

Neutron Reflectivity

Specular reflectivity measurements were performed on the NG7 neutron reflection spectrometer at the National Institute of Standards and Technology with a wavelength (λ) of 4.76 Å and a $\Delta\lambda/\lambda$ value of 2.5%. NR profiles were obtained as a function of wave-vector transfer $q_z = 4\pi\sin\theta/\lambda$, where θ is the angle of incidence and reflection of the neutron beam with the silicon-solvent interface. The high-pressure cell, described in chapter one, was designed and built by High Pressure Equipment Co. (Pennsylvania) specifically for these experiments. The incident neutron beam entered through one sapphire window in the cell, transverses through the edge of the silicon single crystal, reflected from the silicon-polymer-solvent interface with the reflected beam through the crystal again and finally exited through the opposite window to the detector. The stabilities of the temperature and pressure of the cell were ± 0.1 °C and ± 0.2%, respectively. The isothermal condition at 36 °C was maintained over pressures ranging from 0.1 to 14 MPa for the PFA-C_8 brushes. After each pressure change, the exposure time before data collection was approximately 1 h. The time necessary to collect the NR profiles, ranged between 50 to 80 minutes. The background scattering from pure CO_2 was also recorded simultaneously as a function of pressure because it is known to be a measure of the density fluctuations After subtracting the background scattering intensity, we analyzed the data by comparing the observed reflectivity profiles with calculated ones based on model density profiles with three fitting parameters - film thickness, scattering length density (SLD), and interfacial roughness between the polymer and CO_2 - assuming a hyperbolic-tangent density function at the interface[2]. To fit the data, a three layered model was compiled consisting of native silicon oxide (SiOx), PFA-C_8 brush layer, and solvent atmosphere. The real space density profiles were constructed with optimized fit parameters to best fit the data. The density profile PFA-C_8 brush was generated from

$$\phi(z) = \phi s[1-(z/h)^2]^{\alpha}, z < h, \qquad (2.1)$$
$$\phi(z) = 0, z > h,$$

where the main fit parameters are ϕs the polymer volume fraction at the silicon oxide surface, h the cutoff thickness of the profile, and α the "profile exponent" .

2.3 Results and Discussion

2.3.1 Neutron Reflectivity. Neutron scattering length density (NSLD) profiles were constructed from the best fits of the NR profiles seen in Figure 1. These profiles were subsequently converted to polymer volume fraction profiles. The NSLD of the binary mixture PFA-C_8 /CO_2 system is defined by

$$(\text{NLSD})_{\text{mix}}(z) = \phi(z)_{\text{PFA-C8}}(\text{NSLD})_{\text{PFA-C8}} + (1 - \phi(z)_{\text{PFA-C8}})(\text{NSLD})_{\text{CO2}} \qquad (2.2)$$

here $(\text{NSLD})_{\text{mix}}(z)$ is the NSLD of the mixture at a distance z from the substrate, $(\text{NSLD})_{\text{PFA-C8}}$, and $(\text{NSLD})_{\text{CO2}}$ are the pure component NSLD's of PFA-C_8 and CO_2, respectively, and $\phi(z)$ PFA-C_8 is the volume fraction of PFA-C_8 at a distance z from substrate. To ensure conservation of mass, the volume fraction profiles are calculated such that same amount of grafted polymer remains at all solvent concentrations. The resulting profiles can be seen in Fig. 2-1. At the initial atmospheric conditions, the NR profiles could be simply fit using a step function, where α ~0. This suggests a highly concentrated, uniform profile throughout the thickness of the brush in a non-solvent. However, because of the solubility of PFA-C_8 in CO_2, it was not possible to satisfactorily fit the full set of data points under varying solvent densities using a simple step function. Consequently, under CO_2 conditions, it was necessary to introduce a "tail" to the profile in order to fit the data. The tail is modeled using a convolution of a normalized Gaussian of full width at half maximum Δ (tail width) in a region spanning nearly ± 2 Δ about the cutoff length. The volume fraction profiles indicate that as the CO_2 density increases, the regions near the solvent/brush interface become more parabolic in shape as the brush dissipates into the solvent. Good fits were obtained with uniform concentrations in the polymer layer for the non-solvent condition and no preferential adsorption of either CO_2 or polymer at the Si substrate.

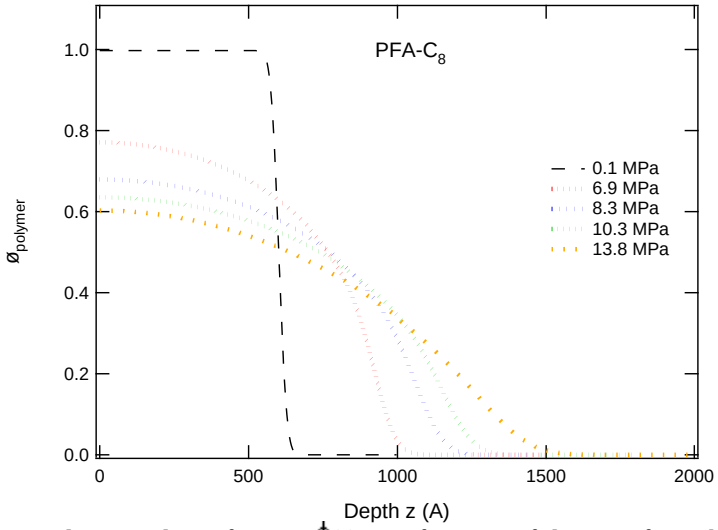

Figure 2-1. Polymer volume fraction $\Phi(z)$ as a function of distance from the grafting surface in air and in CO_2 at 6.9 MPa, 8.3 MPa, 10.3 MPa, and 13.8 MPa, under isothermal conditions (36 C)

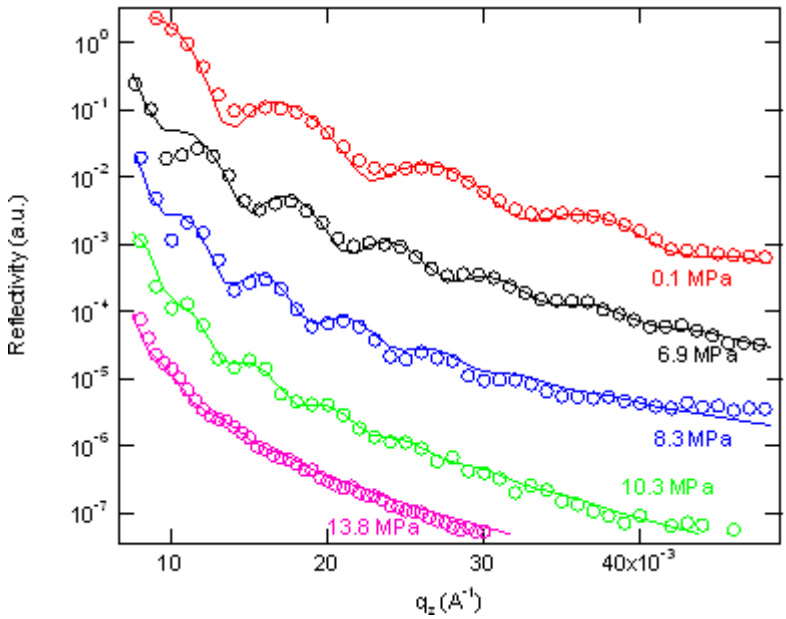

Figure 2-2. Neutron reflectivity profiles under isothermal conditions (36 C) for PFA-C_8 in air and in CO_2 at 6.9 MPa, 8.3 MPa, 10.3 MPa, and 13.8 MPa. For clarity, the profiles are offset by various orders of magnitude.

2.3.2 Brush Swelling. Next, we consider the overall brush swelling with varying solvent quality. Figure 2-2 shows the experimental neutron reflectivity profiles from the brush in a poor solvent (air) and in a good solvent (CO_2) in a pressure range between 6.9 and 13.8 MPa at isothermal conditions (36 C). From the reflectivity profile, the brush height (h) can be estimated $h \sim 2\pi/\Delta q$, where Δq is the distance between successive peak oscillations, for both the dry thickness of the brush and in CO_2 atmosphere. For the non-solvent case of a dry brush in air, the brush height h is ~600 Å. It is evident from the reflectivity that the separation distances of the fringes decrease subsequent to exposure to the solvent. This occurrence is noticeable at all of the generated pressures, with Δq decreasing at each elevated pressure experiment. From the estimation, the brush height increases or swells as a result of $scCO_2$ exposure. The corresponding heights the PFA-C_8 brush, calculated from the best fit of the NR profiles changed to 950 Å at 6.9 MPa, 1100 Å at 8.3 MPa, 1200 Å at 10.3 MPa, and 1400 Å at 13.8 MPa. Near the bulk theta pressure of CO_2, the brush height h_θ ~ 1100 Å. This pressure closely corresponds to the maximum CO_2 density fluctuation at 36 C. The thicknesses of the PFA-C_8 brushes normalized by its theta value h/ h_θ, attained from the best fit of NR profiles, are plotted as a function of the reduced pressure variable, $\rho = (P - \theta) /P$, shown in Figure 2-3.

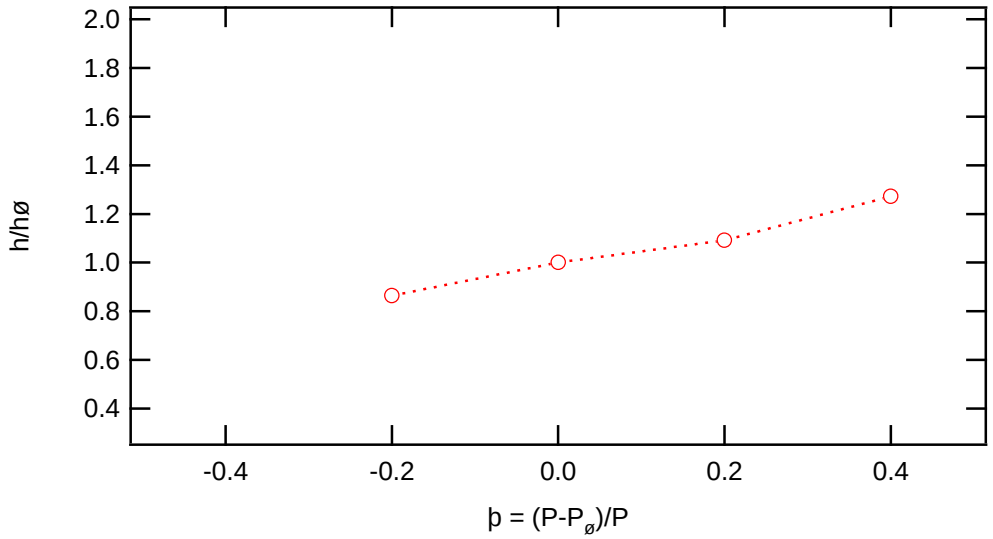

Figure 2-3. Solvent quality dependence of brush height normalized by its θ value, h_θ = 1100 Å in reduced pressure parameters, ρ. Here ρ_θ = 8.3 MPa corresponds to the brush height at approximately the θ value.

Figure 2-4 shows the pressure dependence of linear dilation (*S*f) for the PFA-C_8 brush, which was calculated with the equation $S_f = (L - L_0)/L_0$, where L and L_0 are the measured thicknesses of the swollen and unswollen polymer brushes, respectively. From the figure, a noticeable anomalous peak is present at the density fluctuation ridge. The degree of excess swelling however is less significant compared to previous studies that show very large anomalous swelling behavior for CO_2 insoluble films. One possible explanation for the small excess swelling is that CO_2 penetration is hindered by the semi-crystalline nature of PFA-C_8. Near the surface of film, PFA-C_8 exhibits a high density area where molecular chains assemble in hexagonal packing normal to the substrate[5]. The rigid structures at the surface are likely to perturb the anomalous swelling at the density fluctuation ridge as it has been shown that this phenomenon is principally a surface effect.

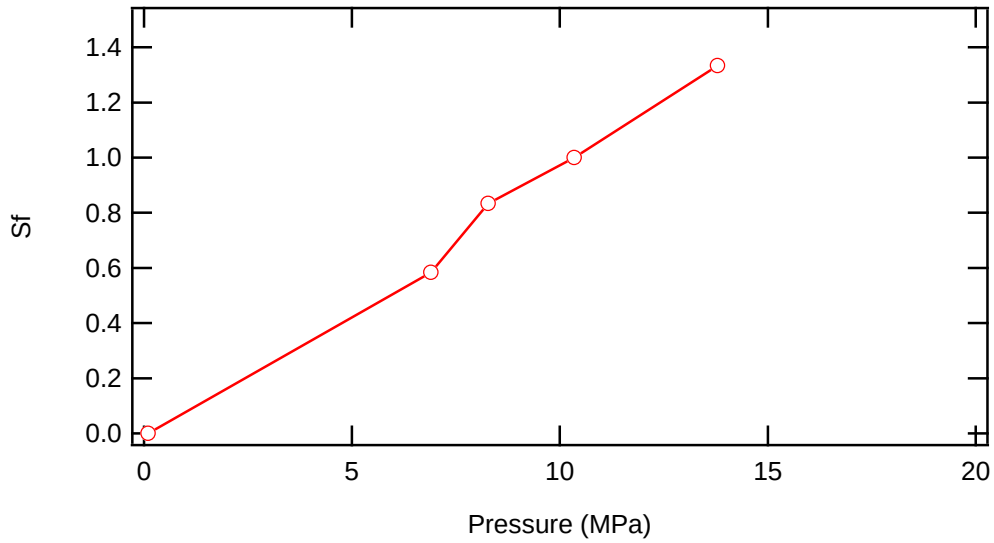

Figure 2-4. Pressure dependence of Sf for PFA-C_8 brush at T = 36 °C

At higher pressures, where density fluctuations can be ignored, the PFA-C_8 chains extend over 100% from their initial thickness. Qualitatively, this means that the polymer chains are extending themselves to maximize favorable contacts with the atmosphere. For immiscible polymers, the films remain collapsed away from the ridge, even at high pressures. Therefore, by increasing by the CO_2 pressure, the density is elevated, resulting in increased solvent quality for PFA-C_8. It is noteworthy that reducing the solvent quality to $\alpha \sim 0$ by depressurization of CO_2, causes contraction of the brush back to the dry thickness, which suggest a reversible swelling phenomenon.

According to the self-consistent field (SCF) theory [6, 7], in the limit of infinitely long chains, for a good solvent the profile exponent $\alpha = 1$ and for a θ solvent $\alpha = 0.5$. We see Fig 2-5, as the concentration of CO_2 increases, the value of α increase from $\alpha \sim 0$ (in air) past $\alpha = 0.5$ and approach $\alpha = 1.0$. Solvent quality improves at 6.9 MPa, but remains in the poor solvent regime. Near theta-solvent conditions are reached at 8.3 MPa and tend towards the good solvent regime when the CO_2 pressure is at 10.3 MPa. At 13.8 MPa, the highest pressure where specular reflectivity fringes are still noticeable, $\alpha = 0.8$. As the density of CO_2 increases beyond this point, the large roughness at the solvent/brush interface hinders specular reflection such that no recognizable fringes necessary to fit the profiles are present.

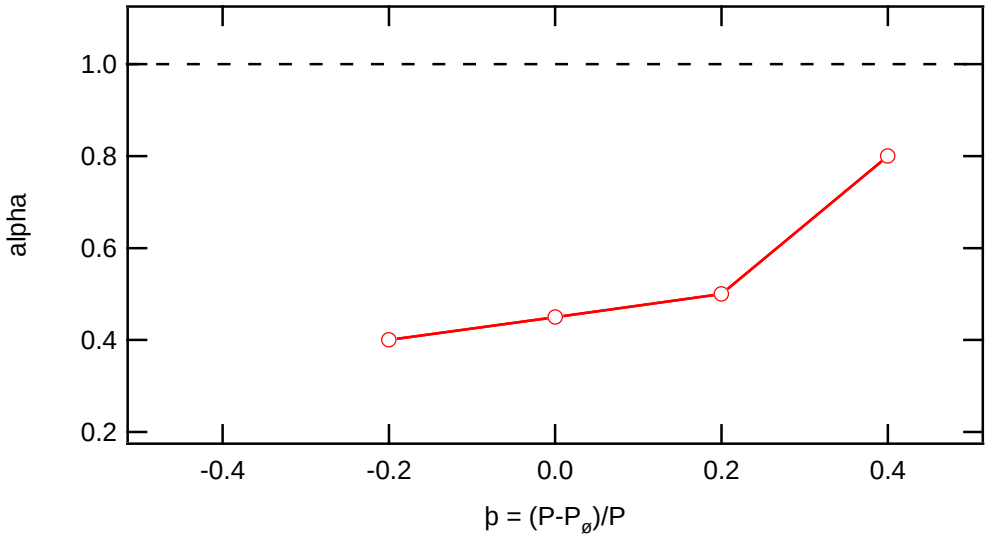

Figure 2-5. Variation of profile exponent α as a function of the reduced pressure variable ρ. The horizontal dashed line corresponds to the SCF prediction of α for a good solvent.

2.3.3 Interfacial Structure. Finally, we discuss the variation of the tail or interfacial width as a function of solvent quality. Figure 2-6 depicts the solvent quality dependence of the normalized interfacial width (Δ/Δ_θ). Near the theta pressure of CO_2, the width of the brush tail, $\Delta_\theta \sim 65$ Å. Under non-solvent conditions, the interface between the solvent and brush is sharp, $\Delta \sim 21$ Å. This is consistent with the numerical calculations of the SCF lattice model, which states that the shape of the brush profile in a poor solvent is box like. Qualitatively, this means that there is not enough attraction between the polymer and solvent to overcome the interchain interactions. As a result, the brush does not diffuse into the solvent, but rather remained concentrated uniformly

throughout the profile. Conversely, as the CO_2 pressure and thus solvent quality increased, the parabolic tail encompassed a larger portion of total brush width due to strong interaction between the chains and solvent. This leads to a diluted interface and less distinguishable brush and CO_2 regions. The width of brush tail is very sizable in the good solvent regime. The large interfacial width at higher CO_2 densities indicates that PFA-C_8 is soluble in CO_2.

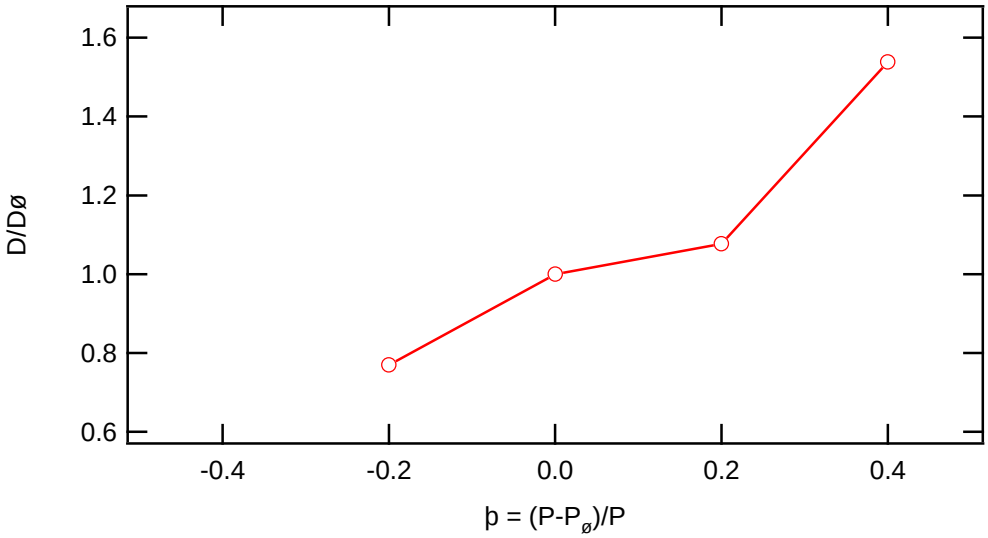

Figure 2-6. Solvent quality dependence of brush interfacial width Δ normalized by its θ value as a function of the reduced pressure variable, ρ. Here Δ_θ = 65 Å corresponds to the brush height at approximately the θ value.

2.4 Conclusion

The swelling behavior and density profiles of end-grafted PFA-C_8 brush in supercritical CO_2 were measured using in-situ neutron reflectivity. By varying the CO_2 density, the solvent quality was tunable over a nearly complete range from non-solvent conditions, past θ-solvent, and into the good solvent regime. As the solvent quality improved, the polymer volume fraction profiles subsequently evolves from block profiles to more parabolic profiles as the non-tethered chain ends extend into the solvent to maximizes favorable contacts. The thicknesses and interfacial widths also increase as the CO_2 densities increase. The extents of these changes are much more significant than for previous studies of polymer brushes in compressible solvents because of the miscibility of PFA-C_8 in CO_2. The tethered ends of the brush also contribute to maximum chain extension, as the polymer chains can stretch without being removed from the substrate unlike the free-chain situation in $scCO_2$. However, the anomalous swelling at the density ridge is suppressed by crystalline structures near the surface of the film. Further study of this observation will be presented in the following chapters.

Reference:

[1] S. M. Sirard, R. R. Gupta, T. P. Russell, J. J. Watkins, P. F. Green, and K. P. Johnston, Macromolecules **36** (9), 3365 (2003).

[2] A. Karim, S. K. Satija, J. F. Douglas, J. F. Ankner, and L. J. Fetters, Physical Review Letters **73** (25), 3407 (1994).

[3] T. Koga, Y. Ji, Y. S. Seo, C. Gordon, F. Qu, M. H. Rafailovich, J. C. Sokolov, and S. K. Satija, Journal of Polymer Science Part B-Polymer Physics **42** (17), 3282 (2004).

[4] J. Kim and R. G. Carbonell, Journal of Supercritical Fluids **42** (1), 129 (2007).

[5] H. Yamaguchi, K. Honda, K. Kobayashi, M. Morita, H. Masunaga, O. Sakata, S. Sasaki, and A. Takahara, Polymer Journal **40** (9), 854 (2008).

[6] S. T. Milner, T. A. Witten, and M. E. Cates, Macromolecules **22** (2), 853 (1989).

[7] E. B. Zhulina, O. V. Borisov, and L. Brombacher, Macromolecules **24** (16), 4679 (1991).

Chapter 3: Introduction of molecular scale porosity into semicrystalline polymer thin films using supercritical carbon dioxide

We report supercritical carbon dioxide _scCO2_ technology used for forming a large degree of molecular scale porosity in semicrystalline polymer thin films. The following three steps were integrated: (i) pre-exposure to an organic solvent which melted crystalline structures but did not cause a decrease in thickness, (ii) scCO2 exposure under the unique conditions where the anomalous absorption of CO2 occurred, and (iii) subsequent quick evaporation of CO2 to preserve the swollen structures. This unified process resulted in homogenous low-density polyphenylene vinylene films (a 15% reduction in density) with the sustained structure for at least 6 months at room temperature.

3.1 Introduction

With the continuous drive and demand for higher performance integrated circuits coupled with increased portability requirements, novel approaches towards the development of new low-dielectric constant (low-*k*) materials must be investigated. According to the National Technology Roadmap, the next generation of interlayer dielectric materials for microelectronics must have an ultra low-dielectric constant (k<2.0) with thicknesses of less than 650 Å[1]. In addition, the materials must meet the stringent process and reliability requirements such as thermal stability, good mechanical properties, good adhesion, etc. Excluding the incorporation of fluorine to lower material's polarity, the only way to achieve such low-*k* is by lowering the density of the materials by introducing nanometer sized pores into an initially low-*k* material [2-5].

Recently, we have developed a new "green" process to create low-density amorphous polymer thin films with a large degree of molecular scale porosity using supercritical carbon dioxide ($scCO_2$, T_c = 31.3 °C and P_c = 7.38 MPa)[6]. The formation of the low-density films have been achieved by the novel features of $scCO_2$: (i) anomalous expansion of the spun-cast films induced by density fluctuations near the critical point of $scCO_2$[7], and (ii) subsequent quick evaporation of CO_2 with the polymer thin films in the vitrified state to preserve the swollen strucutures[6]. In addition, the latter one enables us to dry the film completely, leading to the "non-solvent" process for polymer thin films. Hence, the $scCO_2$ process offers us to create the molecular scale porosity near room temperature without further processing of the polymer with corrosive solvents or heat treatments that may oxidize the polymer or damage the substrate.

The object of this chapter aims to further extend the developed $scCO_2$ process to semicrystalline polymers, which are much more robust and resistant to degradation than amorphous homopolymer films, and to produce new ultra low-k polymer thin films needed for future microelectronics. The challenge is that the solubility of $scCO_2$ with semicrystalline polymers is typically poor due to rigid crystalline structures that prevent CO_2 molecules from penetrating into a polymer matrix[8,9]. To overcome the preventive nature of the crystalline structures, we redesigned the $scCO_2$ process by optimizing "pre-exposure" to an organic solvent that facilitates the melting of crystalline structures allowing CO_2 molecules to fully penetrate and diffuse throughout the film, but does not dissolve the polymer. In addition, if the organic solvent can be dissolved in $scCO_2$, it can be completely removed from the film by the same quick evaporation of $scCO_2$.

3.2 Experimental Section

The model semicrystalline polymer used was poly-phenylene vinylene (PPV) due to its initial low-k (k=2.6), high temperature stability (up to 450°C in N_2 ambient) and easy film preparation. PPV thin films were prepared via chemical vapor deposition (CVD) by vapor phase pyrolysis of α,α'-dibromo-*p*-xylene onto silicon wafers[10]. The conversion of the precursor film was performed by vacuum annealing at T=250°C for measured times (10-40 min). All experiments were initially performed on films with a measured thickness of approximately 400 Å. For PPV films, toluene (≥95% A.C.S. reagent) was chosen as the pre-exposure solvent for its inability to dissolve PPV quickly, and its ability to dissolve in $scCO_2$ readily[11]. As will be discussed later, we found that the pre-exposure time of 1 hour was adequate for our purpose. The films after the pre-exposure were then quickly placed into the high-pressure cell and exposed to $scCO_2$ for 24 h under the

density fluctuation ridge condition (T = 36 ºC and P = 8.2 MPa), where the anomalous excess swelling is induced[6,7], and subsequently depressurized to atmospheric pressure within 10 s to preserve the swollen structures of the polymer films using the vitrification process (T_g ~ 220ºC).

3.3 Results and Discussion

Firstly, we demonstrate the validity of toluene as the pre-exposure solvent. A grazing incidence diffraction (GID) technique, which is sensitive to crystalline structures within a film, was utilized for this purpose. The GID measurements were conducted at the x10B beamline of the National Synchrotron Light Source (NSLS), Brookhaven National Laboratory (BNL) using a photon energy of 14 keV, i.e., x-ray wavelength (λ) of 0.87Å. Figure 1 shows the GID profiles before and after pre-exposure to toluene. The pre-exposure was carried out just before the GID experiments. The glancing angle of incidence was set to 0.2°, which is just above the critical angle of ~0.14° for PPV, in order to determine the crystal structure within the entire film. Prior to immersion in toluene, we could see the multiple Bragg peaks assigned to (110), (210), (120), and (410) lattice planes, indicating the existence of the crystalline domains within the film[12]. However, when the sample was pre-exposed to toluene, this definitive crystal structure was no longer recognizable in the GID profile, as shown in Fig. 3-1. In addition, ellipsometry results proved no changes in the film thickness between the pre-exposed and unexposed films. It should be noted that longer pre-exposure times of more than 3 h caused a slight decrease in the film thickness, indicating that the film was partially dissolved. Consequently, we set the pre-exposure time for the PPV films to be 1 h to melt the crystal structures completely, but not to affect the film thickness.

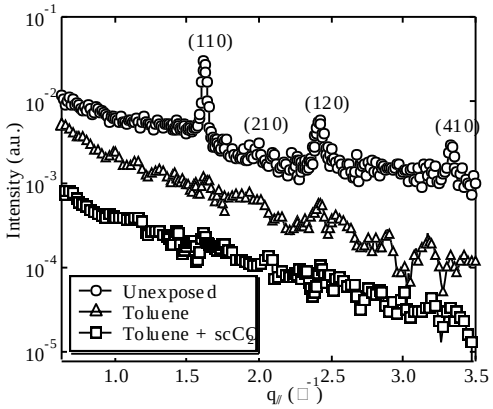

Figure 3-1. GID profiles for the PPV films without and with toluene exposure, and the film (III). The (hk0)s correspond to the miller indices for the PPV crystal structure.

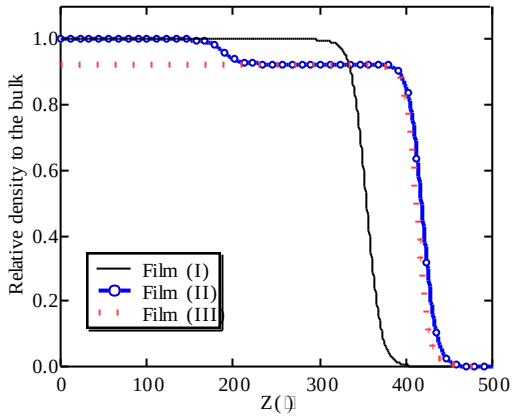

Figure 3-2. Density profiles of the films (I), (II) and (III) obtained from the best-fits to the XR data.

Next, we discuss the effect of the pre-exposure to the $scCO_2$ treatment by using X-ray reflectivity (XR) measurements performed at the same NSLS beamline. Fig. 3-2 summarizes the density profiles for the as-prepared film without pre-exposure, hereafter defined as "film (I)", the film with

exposure to only $scCO_2$, hereafter defined as "film (II)", and the film with the unified process (i.e., the combination of toluene and $scCO_2$ exposure), hereafter defined as "film (III)"[13]. The dispersion (δ) value in the x-ray refractive index obtained from the best-fits to the XR data, which is proportional to the density of a film, was converted into the density of the film relative to the bulk by using the measured dispersion value of the untreated PPV film (δ=1.37×10^{-6}). In the case of the film (II), the initial thickness, L_0= 350 Å, has increased to L=450 Å, which corresponds to a linear dilation, $S_f = (L-L_0)/L_0$=0.20. At the same time, the film has a low-density layer of approximately 200 Å formed at the polymer/air interface, corresponding to a 15% decrease in the density compared to the untreated one or the bulk with a relatively sharp interface of approximately 40 Å and a uniform layer of bulk density beneath. Thus, it is clear that the penetration depth of density fluctuating $scCO_2$, which causes the anomalous swelling, is limited to the surface area. On the other hand, we found that the density of the film (III) decreased by 15%, whose magnitude was the same as the film (II), but *throughout* the entire film. This enhanced penetration power of $scCO_2$ is attributed to the melting of the crystalline regimes in the film. In addition, atomic force microscopy (AFM) images in a series of $100\times100\mu m$ scans across the film (III), as seen in Fig. 3-3, proved that the surface appeared flat with the root-mean-square (rms) roughness of approximately 30 Å between the polymer and air layer, which is consistent with the XR result which gave us the rms roughness of 21 ± 4 Å. Furthermore, small-angle x-ray scattering (SAXS) experiments with reflection geometry, which is a powerful tool used to characterize pore-size distributions at the nanometer scale[14], showed no significant differences in the SAXS profiles between the films (I) and (III) (the data is not shown here). Hence, we postulate that a large degree of molecular scale porosity, which can't be detected by these experimental techniques, is introduced into the entire film with the unified process, leading to the formation of the homogenous low-density PPV film. It should be emphasized that the unified process used for this study allowed us to create homogenous PPV films with thicknesses of up to 700 Å.

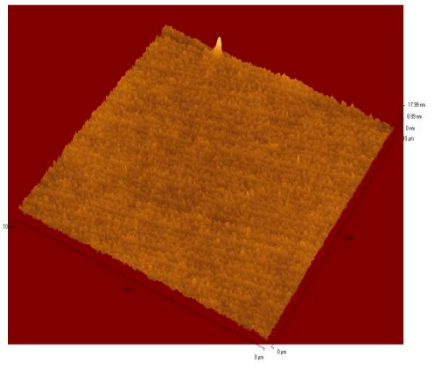

Figure 3-3. AFM 3-dimensional images show a flat surface absent of large voids and pores.

Finally, we discuss the physical, mechanical, and thermal properties of the homogenous low-density PPV film. It is known that a reduction in density of an amorphous polymer is associated with reductions in index of refraction (n_f). As shown in Fig.1, we confirmed that the low-density PPV film (III) did not have any crystalline structures within the film. We therefore measured the changes in optical and electrical properties by using a VASE Research Spectroscopic Ellipsometer (M-44, J.A. Wollam Co, Lincoln, NE) based on a biaxial Cauchy model[15]. Figure 3-4(a) shows the indices of refraction for the films (I) and (III). From the figure we can see that there is a significant decrease (12%) in n_f for the film (III) over the entire range of the wavelength (600 nm–742 nm). Interestingly, this change corresponds to a 23% dielectric constant decrease owing to the relationship of $k \sim n_f^2$. Therefore, we can conclude that relative to the bulk (k~2.6), the low-density PPV film (III) has the low-k value of ~2.0.

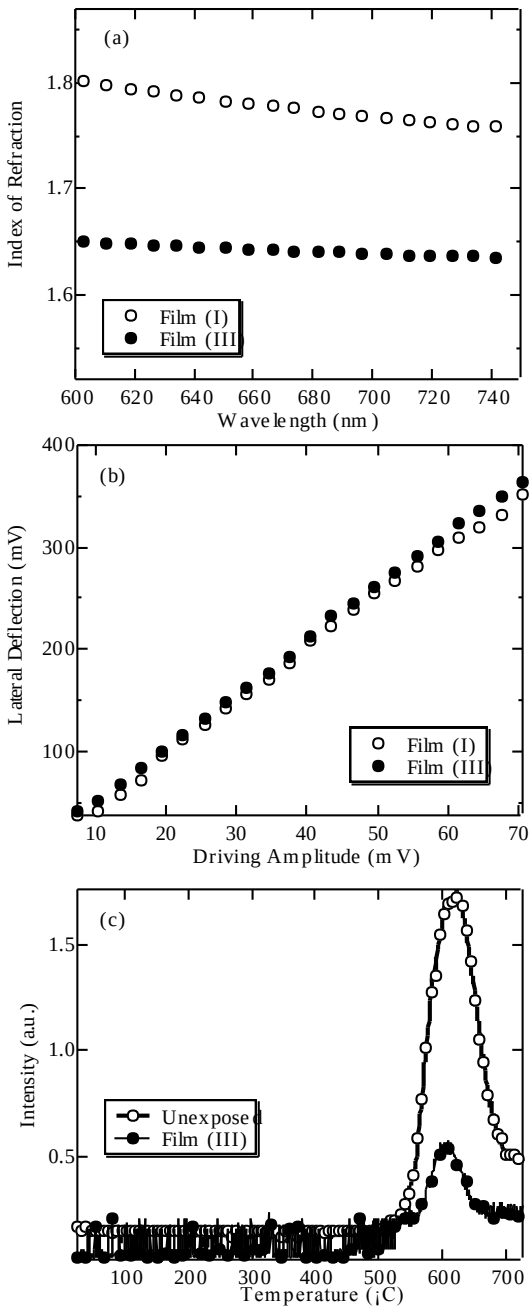

Figure 3-4. Optical, mechanical, and thermal properties of the low-density PPV (III): (a) Index of refraction vs. wavelength; (b) Lateral deflection (ΔX) vs. the drive amplitude; (c) Continuous mass spectra of toluene fragment mass taken during temperature ramping. Note that the untreated sample exhibits the higher intensity because of the larger initial thickness of the prepared film (650 Å).

The advantage of introducing molecular level porosity is the ability to maintain the material's inherent mechanical properties. To investigate the mechanical properties of the low-density film, shear modulation force microscopy (SMFM)[16] using a Digital Instruments Dimension 3000 (Veeco Co. Plainview, NY) was utilized. Figure 3-4(b) shows the lateral deflection (ΔX) of the films (I) and (III) as a function of the driving amplitude at room temperature[17]. It is clear that there is no change in the slope, which corresponds to the surface modulus of the film[16], between the films (I) and (III). Consequently, it is reasonable to conclude that the porosity introduced has no sacrificial effect on the mechanical properties of the low-density PPV film.

The thermal degradation property of the film (III) was also studied by means of *in situ* Mass spectroscopy using MILA-3000 mini lamp cold wall annealing system (ULVAC/Sinku-Riko, Inc., Chigasaki, Japan) connected to a differentially pumped Residual Gas Analyzer RGA-300 (Stanford Research Systems Inc., Sunnyvale, CA)[10]. Figure 3-4(c) shows the spectra for the unexposed film and film (III) taken during dynamic heating at a rate of 20 °C/min up to 800 ºC. A large peak in intensity indicates the release of significant amounts of toluene owing to the film degradation[10]. Thus, the peak initiation (approximately at 500°C) remains unchanged before and after the unified process, proving that the low-density film (III) still imparts the high thermal stability inherent to the material.

3.4 Conclusion

With the novel methodology of using supercritical carbon dioxide as a green solvent, a significant reduction in the dielectric properties of PPV films was achieved. We found that molecular level porosity introduced in the film is responsible for the reduction in density, optical index of refraction, and dielectric constant, but does not

influence the high performance thermal and mechanical properties. We believe that this unified $scCO_2$ process could be relevant to all polymers regardless of the degree of crystallinity, facilitating the use of $scCO_2$ for the formation of molecular scale porosity to be used as scaffolds for interdisciplinary applications as well.

This work was supported by the SRC-NY CAIST funding (2005-KC-1292-012). We thank Drs. Li and Rafailovich for the mechanical property experiments.

3.4 References & Notes

[1] The International Technology Roadmap for Semiconductors. 2008.

[2] J. L. Hedrick, R. D. Miller, C. J. Hawker, K. R. Carter, W. Volksen, D. Y. Yoon, and M. Trollsas, Adv. Mater. **10**, 1049 (1998).

[3] H. J. Lee, E. K. Lin, B. J. Bauer, W. L. Wu, B. K. Hwang, and W. D. Gray, Appl. Phys. Lett. **82**, 1084 (2003).

[4] M. S. Silverstein, M. Shach-Caplan, B. J. Bauer, R. C. Hedden, H. J. Lee, and B. G. Landes, Macromolecules **38**, 4301 (2005).

[5] H. J. Lee, C. L. Soles, D. W. Liu, B. J. Bauer, E. K. Lin, and W. L. Wu, J. Appl. Phys. **100**, (2006).

[6] T. Koga, Y. S. Seo, J. L. Jerome, S. Ge, M. H. Rafailovich, J. C. Sokolov, B. Chu, O. H. Seeck, M. Tolan, and R. Kolb, Appl. Phys. Lett. **83**, 4309 (2003).

[7] T. Koga, Y. S. Seo, Y. M. Zhang, K. Shin, K. Kusano, K. Nishikawa, M. H. Rafailovich, J. C. Sokolov, B. Chu, D. Peiffer, R. Occhiogrosso, and S. K. Satija, Phys. Rev. Lett. **89**, (2002).

[8] Y. Li, E. J. Park, K. T. L. Lim, K. P. Johnston, and P. F. Green, J. Polym. Sci. Part B: Polym. Phys. **45**, 1313 (2007).

[9] E. Weidner, V. Wiesmet, Z. Knez, and M. Skerget, J. of Supercrit. Fluids **10**, 139 (1997).

[10] C. A. Gedelian, G. A. Ten Eyck, and T. M. Lu, Synth. Met. **157**, 48 (2007).

[11] A. Laitinen, Helsinki University of Technology, 2000.

[12] G. Mao, J. E. Fischer, F. E. Karasz, and M. J. Winokur, J. Chem. Phys. **98**, 712 (1993).

[13] It should be added that based on the Fourier Transform (FT) analysis method for XR, the films (I) and (III) could be well described as a single homogenous layer, while the film (II) was approximated as two layers with different densities. The detailed procedure has been described in Ref. 6. Hence, a three-layer model, i.e., a silicon substrate, a native oxide layer and a PPV layer for the films (I) and (III), and a four-layer model with the addition of another PPV layer with a different density to the three layer model for the film (II) were used to analyze the XR data.

[14] K. Omote, Y. Ito, and S. Kawamura, Appl. Phys. Lett. **82**, 544 (2003).

[15] In order to fit the data, the same three-layer model used for the XR analysis was utilized with the literature n_f values for the native oxide layer and Si substrate. Since the film thicknesses of both PPV and SiO_2 layers could be determined by XR, the only floating parameter was the n_f value of the PPV layer.

[16] Y. Ji, B. Q. Li, S. R. Ge, J. C. Sokolov, and M. H. Rafailovich, Langmuir **22**, 1321 (2006).

[17] A small fixed sinusoidal drive signal was applied to the piezo in the direction perpendicular to the scan direction, inducing a small oscillatory motion of the cantilever tip parallel to the polymer surface. At the same time, a normal force was applied to maintain the tip contact with the sample. The lateral deflection amplitude of the cantilever on the polymer surface is measured using a lock-in amplifier, tuned to the drive frequency.

Chapter 4: Conclusions and Recommendations for Future Work

In closing, a summary of the results of the research is presented. Observations that were made along the way will seed the growth of future work. Recommendations for future research are proposed.

4.1 Conclusions

The performance of polymer thin films may be categorized in three ways, mechanical, thermal, and electric. It has been shown that, as the film thickness decreases to the order of the polymer's Rg, the properties of the film deviate from the bulk equivalent. Thermal properties such as glass transition temperature, electric and optoelectronic properties such as dielectric constant influence design and fabrication, and ultimately determine the application and performance of the polymer. Structural stability of the thin film is also considered a crucial mechanical property necessary after processing. For the industrial applications, the tolerance for the thickness of the films may fall in the range of only a few nanometers. It is critical that significant changes in film thickness are detected and accounted for. It is ultimately beneficial that polymer thin films remain in an equilibrium state. However, some external influences may prevent this occurring. Traditional polymer processing using organic solvents and vacuum annealing at high temperatures may lead to a thermodynamically non-equilibrium state.

In order for $scCO_2$ to be more widely considered as a valid technique for polymer processing, we must ensure that the enhanced properties are both controllable and maintainable. Ideally this concerns controlling the molecular scale porosity in thin films, and being able to maintain it for the polymers intended application. We have shown that by using $scCO_2$ we can induce molecular level porosity and capture this low density structure by quickly purging the universal solvent from the polymer. Because $scCO_2$ induces polymer chain stretching, the byproduct is a swollen film that is encompassed with residual stresses. As CO_2 is quenched to preserve the structure, stress is encapsulated in the film. Therefore the fabricated product remains in a meta-stable state. Once thermal energy is applied, relaxation of the polymer chains will occur. As a result, the swollen film collapses and tends towards its initial film thickness. This is undesirable because the attained low density properties using $scCO_2$ processing are lost when the film is placed at elevated temperatures. For applications such as low-dielectric films in integrated circuits, it is necessary to have a high level of thermal stability. For these reasons, we must find a way to stabilize and preserve the structures formed using $scCO_2$.

4.2 Future Work

One foreseeable method of stabilizing polymer films at high temperatures is with a cross-linking agent. Cross-linking is a long established method for restricting the mobility of individual polymer chains by chemically joining two or more molecules by covalent or ionic bonds. This process has been used to inhibit the formation of crystalline structures in polymers, and to limit chain extension under loading. Because of this newly formed network of bonds, chemically cross-linked polymers impart higher thermal and mechanical resistance. It may be possible then to cross-link polymer thin films that have been processed in $scCO_2$ in order to prevent the collapse of films at higher temperatures.

This is extremely beneficial for polymer applications, such as integrated circuits, where high thermal and mechanical performance is necessary.

To test the validity of using a cross-linking reagent to preserve the swollen structures initiated by $scCO_2$ in polymer thin films, we must observe the behavior of the films in a high temperature environment. Of particular importance are changes in film's thickness and density because of dependent properties such as electron mobility. From our previous study, we were able to produce an ultra low index of refraction and dielectric constant polymer thin film on an inorganic substrate by using $scCO_2$ as a green solvent. The swelling induced by the solvent created a uniform low density region throughout the entire film. Using X-ray Reflectivity, we can determine changes and thickness and extrapolate the density profiles of the polymer films. We wish to show that even after annealing at high temperatures, the cross-linked films are still homogenous and low density, unlike films that were processed only with $scCO_2$. It is also necessary to show that the mechanical performance of the films is not degraded. This is important from a practical aspect i.e. the use of $scCO_2$ processes for industrial applications.

Our initial experiments were performed on styrenic elastomers, SEBS, poly(styrene-ethylene-butylene-styrene), and SBS, poly(styrene-butadiene-styrene), tri-block copolymers. These polymers exhibit a large degree of excess swelling at the density fluctuation ridge which can be easily preserved when the solvent is removed. The films were spun cast from polymer solutions of varying concentration with a dispersed photoinitiated cross-linker (1 and 10 polymer weight %). The films were exposed to density fluctuating $scCO_2$ for 2 hours to induce swelling. The solvent was quickly removed to freeze the structure of the film. Immediately after, the films were cured under ultraviolet light to polymerize the photoinitator. The samples were subsequently placed in a vacuum oven at temperatures exceeding the glass transition of the polymer to allow the polymer chains to reach configurational equilibrium.

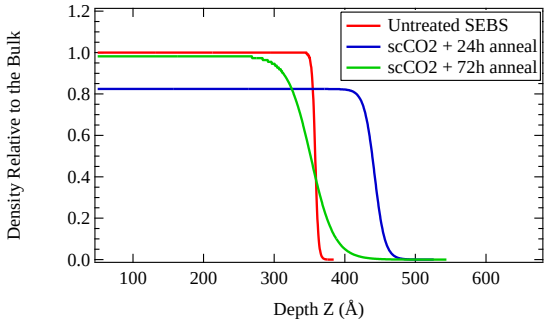

Figure 4-1. Density profiles extrapolated from XR treated above its glass transition temperature (160 °C) for 24 h and 72 h.

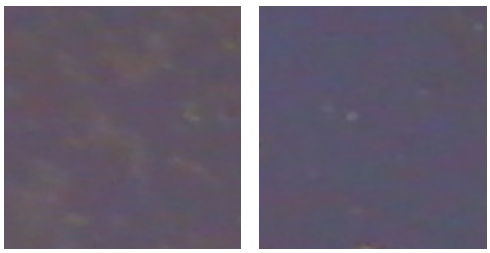

Figure 4-2. (a) SEBS thin film with 1 weight % cross-linker exhibits dewetting structure after 72 h annealing. (b) 10 weight % cross-linker films are homogenous after 72 h annealing

XR measurements for the polymer thin films containing 1 weight % cross-linker showed that even after annealing at high temperatures for 24 h, the films processed with $scCO_2$, are still low density, as seen in Fig. 4-1. However, after longer annealing periods (72 h) the low density layer is less pronounced, and the thickness reduces towards the measured as-spun thickness. Visual inspection also reveals an unstable film, as signs of film "dewetting" are evident, Fig. 4-2(a). In the case of the polymer thin films spun with 10 weight % photoinitiator, no signs of dewetting can be seen visually, Fig. 4-2(b). This difference

may occur because in the first case, (1 weight % cross-linker) there is an insufficient amount of cross-linker to form a strong polymer network. However in the second case, the larger percentage cross-linker allows for increased bonding between polymer chains, and thus a strong network. This occurrence points to a thermally stable film, even at temperatures above the polymer's glass transition for an extended period of time, when the concentration of cross-linker is high. It is important then to perform a more in depth study on the concentration dependence of the cross-linker on the film's temperature stability. Initial studies have also shown that the cross-linker concentration has a significant detrimental effect on the film's swelling behavior, as seen in Fig. 4-3. As a result, we need to optimize the cross-linking process such that the swelling ratio of the film is maximized while keeping the integrity of the film intact at high temperatures.

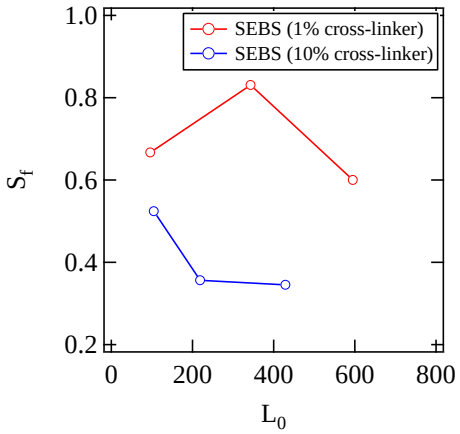

Figure 4-3. Swelling ratios of SEBS thin films containing 1 and 10 weight % cross-linker after exposure to $scCO_2$ for 2 h.

From a practical prospective, the important question arises whether we can use this approach to stabilize other polymers such as PPV to preserve the enhanced properties. It is also important to investigate the influence of these processes to the mechanical properties of the film. Once established, we can unify the entire process (pre-exposure to softening agent, exposure to $scCO_2$, and UV curing) to enhance and sustain the structures of the modified films.

As seen in my previous studies, my greatest interest and goal is to propel SCFs as a valid alternative and technique for polymer processing. We have shown that a wide variety of polymer thin films can swell as much as 30-60 % in density fluctuating $scCO_2$, even when the bulk polymers have very poor miscibility with CO_2 [1]. Because the functional form of the swelling amplitude exactly follows that of the calculated long-range density fluctuations as a function of temperature and pressure, it is believed that the long-range density fluctuations directly control the absolute solubility of supercritical $scCO_2$. The important question arises whether the anomalous solvent quality is universal for all SCFs. This is important from two aspects, one being from an academic point of view, i.e. determining the origins of the anomalous solubility in density fluctuating solvents, and the other from a practical aspect, i.e. determining the feasibility of other SCFs as other universal solvents.

In this regard, we would like to use various supercritical fluids of different molecular composition and molecular interaction to determine the differences in the behavior of density fluctuating SCFs and consequently, the enhanced solvent quality. Of particular interest is supercritical Trifluoromethane ($scCF_3H$, Tc= 26.1 ºC and Pc=4.9MPa) because CF_3H molecules are highly interactive due to a very strong dipole moment (1.65 Debye) [2]. The polymers used in this study will be both glassy, (deuterated polystyrene and deuterated polymethylmethacrylate), and rubbery (deuterated polybutadiene, and deuterated styrene-butadiene random copolymer) films, spun-cast onto Si substrates, in order to make the comparison between the swelling behaviour of these films in non-polar $scCO_2$ [3].

Reference:

[1] T. Koga, Y. S. Seo, Y. M. Zhang, K. Shin, K. Kusano, K. Nishikawa, M. H. Rafailovich, J. C. Sokolov, B. Chu, D. Peiffer, R. Occhiogrosso, and S. K. Satija, Phys. Rev. Lett. 89, (2002)

[2] A. Shariati, K. Gutkowski, C.J. Peters, AIChE J. 51, 1532 (2005).

[3] T. Koga, Y. S. Seo, K. Shin, Y. Zhang, M. H. Rafailovich, J. C. Sokolov, B. Chu, S. K. Satija, *Macromolecules*, *36*, 5236 (2003).

Bibliography

Chapter 1:

[1] Y. Li, X. C. Wang, I. C. Sanchez, K. P. Johnston, P. F. Green, *Journal of Physical Chemistry B* **2007**, *111*, 16.

[2] L. Meli, Y. Li, K. T. Lim, K. P. Johnston, P. F. Green, *Macromolecules* **2007**, *40*, 6713.

[3] J. A. Lubguban, S. Gangopadhyay, B. Lahlouh, T. Rajagopalan, N. Biswas, J. Sun, D. H. Huang, S. L. Simon, A. Mallikarjunan, H. C. Kim, J. Hedstrom, W. Volksen, R. D. Miller, M. F. Toney, *Journal of Materials Research* **2004**, *19*, 3224.

[4] H. Wakayama, Y. Fukushima, *Industrial & Engineering Chemistry Research* **2000**, *39*, 4641.

[5] Y. P. Handa, J. Roovers, F. Wang, *Macromolecules* **1994**, *27*, 5511.

[6] H. Yokoyama, K. Sugiyama, *Langmuir* **2004**, *20*, 10001.

[7] T. Koga, Y. S. Seo, J. L. Jerome, S. Ge, M. H. Rafailovich, J. C. Sokolov, B. Chu, O. H. Seeck, M. Tolan, R. Kolb, *Applied Physics Letters* **2003**, *83*, 4309.

[8] T. Koga, *Kobunshi Ronbunshu* **2004**, *61*, 458.

[9] E. K. Lin, C. L. Soles, D. L. Goldfarb, B. C. Trinque, S. D. Burns, R. L. Jones, J. L. Lenhart, M. Angelopoulos, C. G. Willson, S. K. Satija, W. L. Wu, *Science* **2002**, *297*, 372.

[10] T. Koga, Y. S. Seo, X. Hu, K. Shin, Y. Zhang, M. H. Rafailovich, J. C. Sokolov, B. Chu, S. K. Satija, *Europhysics Letters* **2002**, *60*, 559.

[11] S. M. Sirard, K. J. Ziegler, I. C. Sanchez, P. F. Green, K. P. Johnston, *Macromolecules* **2002**, *35*, 1928.

[12] T. Koga, Y. S. Seo, K. Shin, Y. Zhang, M. H. Rafailovich, J. C. Sokolov, B. Chu, S. K. Satija, *Macromolecules* **2003**, *36*, 5236.

[13] X. C. Wang, I. C. Sanchez, *Langmuir* **2006**, *22*, 9251.

[14] K. Nishikawa, T. Morita, *Chemical Physics Letters* **2000**, *316*, 238.

[15] K. Nishikawa, I. Tanaka, Y. Amemiya, *Journal of Physical Chemistry* **1996**, *100*, 418.

[16] A. Karim, S. K. Satija, J. F. Douglas, J. F. Ankner, L. J. Fetters, *Physical Review Letters* **1994**, *73*, 3407.

[17] S. M. Sirard, R. R. Gupta, T. P. Russell, J. J. Watkins, P. F. Green, K. P. Johnston, *Macromolecules* **2003**, *36*, 3365.

[18] T. Koga, Y. Ji, Y. S. Seo, C. Gordon, F. Qu, M. H. Rafailovich, J. C. Sokolov, S. K. Satija, *Journal of Polymer Science Part B-Polymer Physics* **2004**, *42*, 3282.

[19] J. Burke, in *The book and Paper Group Annual*, Vol. 3, The Oakland Museum of California, Austin **1984**, 13.

[20] Y. Li, E. J. Park, K. T. L. Lim, K. P. Johnston, P. F. Green, *Journal of Polymer Science Part B-Polymer Physics* **2007**, *45*, 1313.

[21] E. Weidner, V. Wiesmet, Z. Knez, M. Skerget, *Journal of Supercritical Fluids* **1997**, *10*, 139.

[22] R. Ivkov, P. D. Butler, S. K. Satija, L. J. Fetters, *Langmuir* **2001**, *17*, 2999.

[23] C. L. Soles, J. F. Douglas, R. L. Jones, W. L. Wu, *Macromolecules* **2004**, *37*, 2901.

[24] S. C. Tucker, *Chemical Reviews* **1999**, *99*, 391.

[25] H. E. Stanley, *Introduction to Phase Transition and Critical Phenomena*, Oxford University Press, Oxford **1971**.

[26] M. H. L. F.H. Huang, K.E. Starling and F.T.H. Chung, *J Chem Eng Jpn* **1985**, *18*, 490.

[27] T. Koga, J. Jerome, M. H. Rafailovich, B. Chu, J. Douglas, S. Satija, *Advances in Colloid and Interface Science* **2006**, *128*, 217.

Chapter 2:

[1] S. M. Sirard, R. R. Gupta, T. P. Russell, J. J. Watkins, P. F. Green, and K. P. Johnston, Macromolecules **36** (9), 3365 (2003).

[2] A. Karim, S. K. Satija, J. F. Douglas, J. F. Ankner, and L. J. Fetters, Physical Review Letters **73** (25), 3407 (1994).

[3] T. Koga, Y. Ji, Y. S. Seo, C. Gordon, F. Qu, M. H. Rafailovich, J. C. Sokolov, and S. K. Satija, Journal of Polymer Science Part B-Polymer Physics **42** (17), 3282 (2004).

[4] J. Kim and R. G. Carbonell, Journal of Supercritical Fluids **42** (1), 129 (2007).

[5] H. Yamaguchi, K. Honda, K. Kobayashi, M. Morita, H. Masunaga, O. Sakata, S. Sasaki, and A. Takahara, Polymer Journal **40** (9), 854 (2008).

[6] S. T. Milner, T. A. Witten, and M. E. Cates, Macromolecules **22** (2), 853 (1989).

[7] E. B. Zhulina, O. V. Borisov, and L. Brombacher, Macromolecules **24** (16), 4679 (1991).

Chapter 3:

[1] The International Technology Roadmap for Semiconductors. 2008.

[2] J. L. Hedrick, R. D. Miller, C. J. Hawker, K. R. Carter, W. Volksen, D. Y. Yoon, and M. Trollsas, Adv. Mater. **10**, 1049 (1998).

[3] H. J. Lee, E. K. Lin, B. J. Bauer, W. L. Wu, B. K. Hwang, and W. D. Gray, Appl. Phys. Lett. **82**, 1084 (2003).

[4] M. S. Silverstein, M. Shach-Caplan, B. J. Bauer, R. C. Hedden, H. J. Lee, and B. G. Landes, Macromolecules **38**, 4301 (2005).

[5] H. J. Lee, C. L. Soles, D. W. Liu, B. J. Bauer, E. K. Lin, and W. L. Wu, J. Appl. Phys. **100**, (2006).

[6] T. Koga, Y. S. Seo, J. L. Jerome, S. Ge, M. H. Rafailovich, J. C. Sokolov, B. Chu, O. H. Seeck, M. Tolan, and R. Kolb, Appl. Phys. Lett. **83**, 4309 (2003).

[7] T. Koga, Y. S. Seo, Y. M. Zhang, K. Shin, K. Kusano, K. Nishikawa, M. H. Rafailovich, J. C. Sokolov, B. Chu, D. Peiffer, R. Occhiogrosso, and S. K. Satija, Phys. Rev. Lett. **89**, (2002).

[8] Y. Li, E. J. Park, K. T. L. Lim, K. P. Johnston, and P. F. Green, J. Polym. Sci. Part B: Polym. Phys. **45**, 1313 (2007).

[9] E. Weidner, V. Wiesmet, Z. Knez, and M. Skerget, J. of Supercrit. Fluids **10**, 139 (1997).

[10] C. A. Gedelian, G. A. Ten Eyck, and T. M. Lu, Synth. Met. **157**, 48 (2007).

[11] A. Laitinen, Helsinki University of Technology, 2000.

[12] G. Mao, J. E. Fischer, F. E. Karasz, and M. J. Winokur, J. Chem. Phys. **98**, 712 (1993).

[13] It should be added that based on the Fourier Transform (FT) analysis method for XR, the films (I) and (III) could be well described as a single homogenous layer, while the film (II) was approximated as two layers with different densities. The detailed procedure has been described in Ref. 6. Hence, a three-layer model, i.e., a silicon substrate, a native oxide layer and a PPV layer for the films (I) and (III), and a four-layer model with the addition of another PPV layer with a different density to the three layer model for the film (II) were used to analyze the XR data.

[14] K. Omote, Y. Ito, and S. Kawamura, Appl. Phys. Lett. **82**, 544 (2003).

[15] In order to fit the data, the same three-layer model used for the XR analysis was utilized with the literature n_f values for the native oxide layer and Si substrate. Since the film thicknesses of both PPV and SiO_2 layers could be determined by XR, the only floating parameter was the n_f value of the PPV layer.

[16] Y. Ji, B. Q. Li, S. R. Ge, J. C. Sokolov, and M. H. Rafailovich, Langmuir **22**, 1321 (2006).

[17] A small fixed sinusoidal drive signal was applied to the piezo in the direction perpendicular to the scan direction, inducing a small oscillatory motion of the cantilever tip parallel to the polymer surface. At the same time, a normal force was applied to maintain the tip contact with the sample. The lateral deflection amplitude of the cantilever on the polymer surface is measured using a lock-in amplifier, tuned to the drive frequency.

Chapter 4:

[1] T. Koga, Y. S. Seo, Y. M. Zhang, K. Shin, K. Kusano, K. Nishikawa, M. H. Rafailovich, J. C. Sokolov, B. Chu, D. Peiffer, R. Occhiogrosso, and S. K. Satija, Phys. Rev. Lett. 89, (2002)

[2] A. Shariati, K. Gutkowski, C.J. Peters, AIChE J. 51, 1532 (2005).

[3] T. Koga, Y. S. Seo, K. Shin, Y. Zhang, M. H. Rafailovich, J. C. Sokolov, B. Chu, S. K. Satija, *Macromolecules, 36*, 5236 (2003).